AIP | Review of Scientific Instruments

Evanescent field: A potential light-tool for theranostics application

Nabarun Polley, Soumendra Singh, Anupam Giri, and Samir Kumar Pal

Citation: Review of Scientific Instruments **85**, 033108 (2014); doi: 10.1063/1.4868589
View online: http://dx.doi.org/10.1063/1.4868589
View Table of Contents: http://scitation.aip.org/content/aip/journal/rsi/85/3?ver=pdfcov
Published by the AIP Publishing

Evanescent field: A potential light-tool for theranostics application

Nabarun Polley,[1] Soumendra Singh,[1,2] Anupam Giri,[1] and Samir Kumar Pal[1,a)]
[1]*Department of Chemical, Biological and Macromolecular Sciences, S. N. Bose National Centre for Basic Sciences, Block JD, Sector III, Salt Lake, Kolkata 700 098, India*
[2]*Centre for Astroparticle Physics and Space Science, Department of Physics, Bose Institute, 93/1, Acharya Prafulla Chandra Road, Kolkata 700 009, India*

(Received 12 November 2013; accepted 3 March 2014; published online 25 March 2014)

A noninvasive or minimally invasive optical approach for theranostics, which would reinforce diagnosis, treatment, and preferably guidance simultaneously, is considered to be major challenge in biomedical instrument design. In the present work, we have developed an evanescent field-based fiber optic strategy for the potential theranostics application in hyperbilirubinemia, an increased concentration of bilirubin in the blood and is a potential cause of permanent brain damage or even death in newborn babies. Potential problem of bilirubin deposition on the hydroxylated fiber surface at physiological pH (7.4), that masks the sensing efficacy and extraction of information of the pigment level, has also been addressed. Removal of bilirubin in a blood-phantom (hemoglobin and human serum albumin) solution from an enhanced level of 77 μM/l (human jaundice >50 μM/l) to ~30 μM/l (normal level ~25 μM/l in human) using our strategy has been successfully demonstrated. In a model experiment using chromatography paper as a mimic of biological membrane, we have shown efficient degradation of the bilirubin under continuous monitoring for guidance of immediate/future course of action. © *2014 AIP Publishing LLC*. [http://dx.doi.org/10.1063/1.4868589]

I. INTRODUCTION

Importance of light in the medical diagnosis and therapy is unanimous. Starting from invention of light microscope in sixteenth century for the pathological use till "bloodless" laser surgery in the twentieth century are the few exemplary evidences.[1–5] Advent of nanotechnology further opens up the scope of light for the diagnosis and therapy. For example, use of quantum dots (QDs) for the early diagnosis and photodynamic therapy of cancer are reported in the literature.[6–8] Potentiality in the use of zinc oxide nanoparticle in the light-assisted treatment of hyperbilirubinemia is also reported from this group.[9] Light as universal excitation source of spectroscopy in optical biopsy is evident in the literature.[10,11] Use of optical fiber in the biomedical instrumentation for guiding light is also found to be another important way for the medical use of light in endoscopy.[12–14] A significant portion of fiber optic-based biosensors relies on the efficient interaction of evanescent field with the environments under investigation.[15–19] Several good reviews on the use and control of evanescent field are reported in the present literature.[17,20,21] The studies are mainly focused on the sensing of biomedically important analytes, aiming to develop novel diagnostic protocol. However, use of evanescent field for a potential therapeutic use is sparse in the literature.[15–23] In one of the application based works, a pad of woven fibers used to transport light from a light source to the neonatal skin through leaky modes for the treatment of neonatal jaundice.[24] Other products for the sensing of variety of physical parameters including oxygen level, pH of a solution, temperature based on fiber optic absorption and fluorescence techniques are also reported in the literature.[25–28] Nonetheless, to the best of our knowledge, use of evanescent field for the simultaneous diagnosis and therapy is absent in the literature and is the motive of present work.

In the present study, we have used evanescent field of a silica fiber for probing a bile pigment bilirubin in aqueous solution. Bilirubin is a metabolic waste product that generally excreted through bile and urine, but for some disease conditions in liver and biliary tract, bilirubin starts to accumulate in tissues and blood, leading to jaundice.[29] Accumulation of bilirubin is very much common in neonates, causing neonatal jaundice. During the first week of life, around half of the all neonates are affected by jaundice.[30] Till date phototherapy is the most effective treatment for neonatal jaundice.[30,31] In phototherapy the neonates are placed under blue light, since, bilirubin absorbs light in the blue region of the optical spectrum.[32–35] In conventional phototherapy, bilirubin level of the patients is recommended to be monitored time to time through blood test, in order to determine the required dosage and future course of action. In this context, a noninvasive/minimally invasive procedure for the phototherapy can be very helpful. In the present study, we have shown that the evanescent field coupled to the aqueous environment can efficiently be used for degradation of bilirubin. Our method offers a strategy for continuous monitoring the level of bilirubin during the degradation process, which is extremely important for the immediate course of action. We have found that deposition of our test pigment bilirubin on the surface of the sensor silica core fiber due to the presence of unavoidable hydroxyl functional groups[26] at physiological pH (~7.4). Apparent masking of the sensitivity of fiber optic biosensors due to deposition and extraction of relevant information have also been addressed in our studies. We have successfully demonstrated our strategy in the removal of clinically significant

a)Authors to whom correspondence should be addressed. Electronic mail: skpal@bose.res.in

amount of bilirubin in blood-phantom solution (hemoglobin and human serum albumin (HSA)). In a model study using chromatography paper as biological membrane mimic, we have established the efficacy of the developed technique, *in vitro*. Briefly, the developed evanescent optical approaches are expected to unite diagnosis, treatment, and potential treatment-guidance in one procedure for the management of hyperbilirubinemia.

II. MATERIALS AND METHODS

All the chemicals including bilirubin (Ixα) used in our studies were received from Sigma Aldrich (USA). Bilirubin was dissolved in water (from Millipore) at pH ~10 to prepare the stock solution. To prepare our test solution we diluted a small portion of this stock solution by water and the final pH of the test solution was adjusted around 7.5 (close to physiological pH). We have used freshly prepared aqueous solution of the test pigment for our experiments. We have used multi-mode silica core fiber (FT200UMT) from Thorlabs (USA). As per the vendor's specifications, the core, clad, and overall diameters of the silica fiber are 200 μm, 225 μm, and 500 μm, respectively. The multi-modal 1000 μm plastic fiber (OMPF1000) used in our studies is from OMC (UK). For the high resolution electron microscopy, we have used scanning electron microscope (SEM) from FEI (Quanta FEG 250). For the spectroscopic studies, we have used Ocean Optics HR4000 spectrograph with a white light source (LS-450) and Shimadzu (Japan) spectrophotometer (UV-2600). Software from Ocean Optics (SpectraSuite) has been used for the data acquisition. We have coupled 1 W blue LED (GP-1WW6-11100-X38T, peak at 450 nm) from Golden Gadgets to the optical fibers with SMA (SubMiniature version A) connector (Thorlabs; 10510A, 11050A) through a fiber coupler (Ocean Optics, 74-UV). In order to monitor power at the end of the optical fibers, we have used nano-watt power meter from Coherent (FieldMate with OP-2 VIS sensor). A peristaltic pump from APT Instruments (Vitton-3) has been used for the recirculation of the aqueous bilirubin solution in our *in vitro* studies. In order to enhance the evanescent fields of the optical fibers we have used manual etching of the fiber clad as reported in earlier works.[17,36] In the case of plastic fiber, we have used thermal etching techniques as described in the literature.[17–19]

In the present work, we have used evanescent field of the optical fibers for the potential theranostics application in hyperbilirubinemia. It has to be noted that the evanescent wave is a near-field wave with an intensity that exhibits exponential decay without absorption as a function of the distance from the core-clad boundary of the optical fiber as shown in Figure 1. The standard practice for the estimation of penetration depth (d_p) of the evanescent field in a "non-absorbing" medium can be illustrated in the following way.[17] In a fiber optic cable the optical signal is transmitted by total internal reflection of the light. The light from the silica core with refractive index n_1 is incident on the clad with refractive index n_2, where $n_1 > n_2$. As a result the light is internally reflected totally, depending upon the incident angle θ, where $\theta > \theta_c$

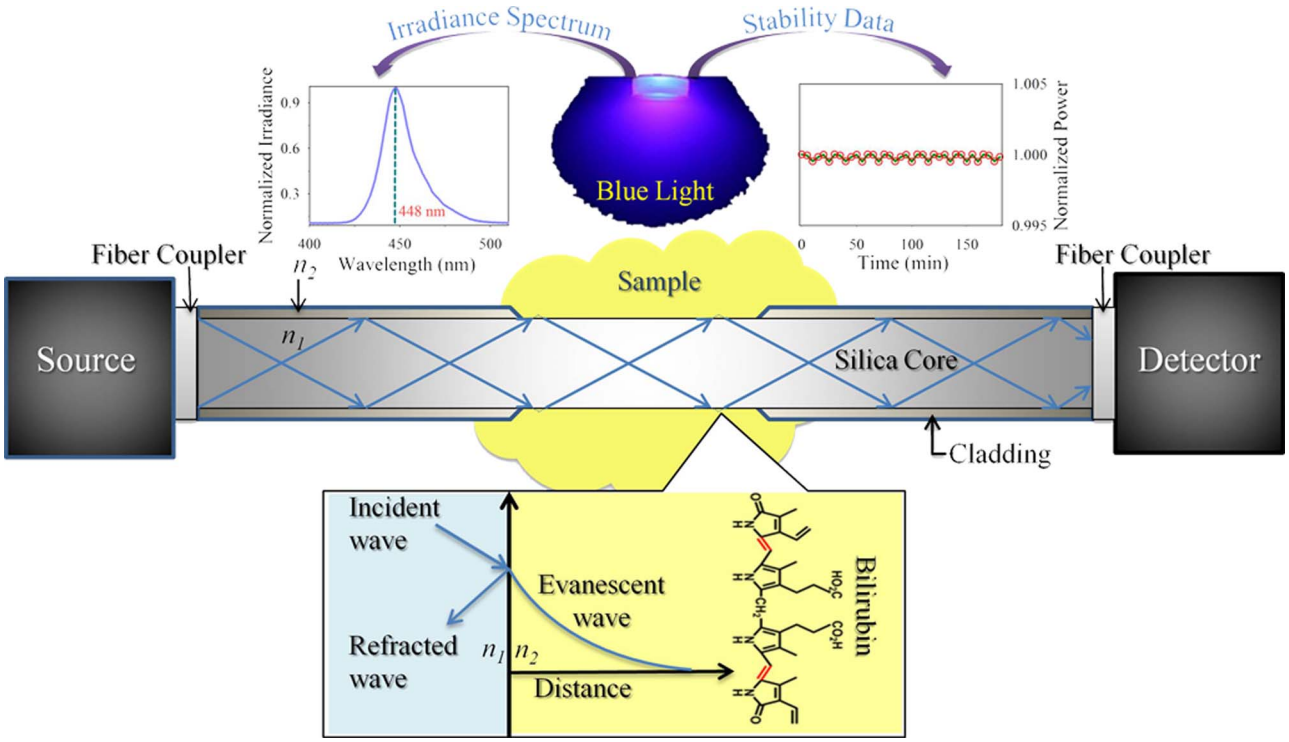

FIG. 1. Schematic representation of our experimental setup. For the spectroscopic monitoring of photodegradation by an external blue LED (of 450 nm wavelength) a white light as "Source" and a spectrograph as "Detector" was used for bilirubin sensing. Potential use of the setup in theranostics application has been demonstrated by replacing the white light with blue LED (source) and optical power meter (detector) at the other end of the fiber, without employing any external light source for photodegradation of bilirubin. The upper insets in left and right represent the irradiation spectra of the LED and its stability, respectively. The lower inset shows mechanistic details of evanescent field for the detection of bilirubin.

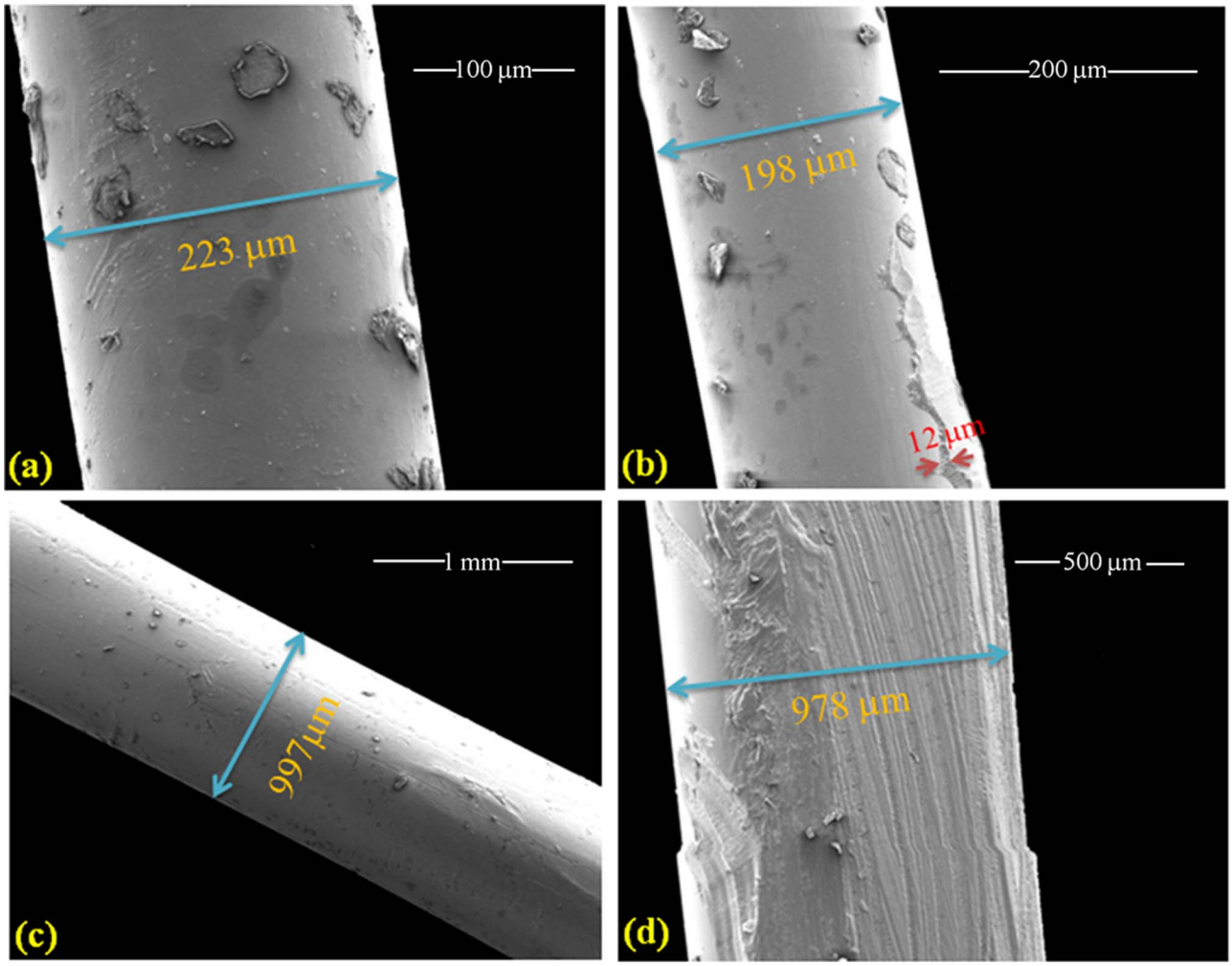

FIG. 2. Scanning electron microscopic image of bare silica (a) and plastic (c) fibers. The modified surface of the silica (b) and plastic (d) fibers after manual etching/heating are also shown.

(θ_c is the critical angle). In practice the light does not reflect back from the exact plane of separation between core and clad, rather it has certain penetration depth in the clad region. The penetration depth or depth of penetration (d_p) is defined as[17]

$$d_p = \frac{\lambda}{2\pi\sqrt{(n_1{}^2 \sin^2\theta - n_2{}^2)}}. \quad (1)$$

The estimated penetration depth for our case is in the range of few hundreds of nm. However, if any portion of clad is removed or etched (as in our case) the depth of penetration would change. It is also worth mentioning that evanescent field strongly interacts with the environment outside the fiber and carry spectroscopic information, and is the key of all the waveguide-based sensors.[17] The scenario would change in the case of an environment, which offers strong optical absorption to the light responsible for the evanescent field.[37,38] This can be conveniently taken into account by defining a complex refractive index,[37]

$$\tilde{n} = n + i\kappa. \quad (2)$$

Here, the real part of the refractive index n indicates the phase speed, while imaginary part κ indicates the amount of absorption loss when electromagnetic wave propagates through the medium. Both the real and imaginary parts of the refractive index are the functions of wavelength of the light propagating through the optical fiber. One way to incorporate attenuation of the evanescent field in the absorbing medium is via an absorption coefficient (α_{abs})[37,38] in the following way:

$$I(z) = I_0 e^{-\alpha_{abs} z}, \quad (3)$$

where I(z) is the intensity of the evanescent field at a distance of z from the interface having field intensity of I_0. α_{abs} denotes absorption coefficient of the medium and equal to twice the magnitude of the imaginary component of the refractive index ($2 \times \kappa$).[37] In this formulation the penetration depth, d_p would be just inverse of the absorption coefficient ($1/\alpha_{abs}$).[37] From the above formulation it is clear that the penetration depth of the evanescent field in an absorbing medium very much depends on the concentration of the analyte in the medium.

For the potential use of the evanescent field in the light therapy, the amount of light (optical power), which is proportional to number of optical modes in the guide fiber, is an important quantity. The number of modes coupled to a fiber

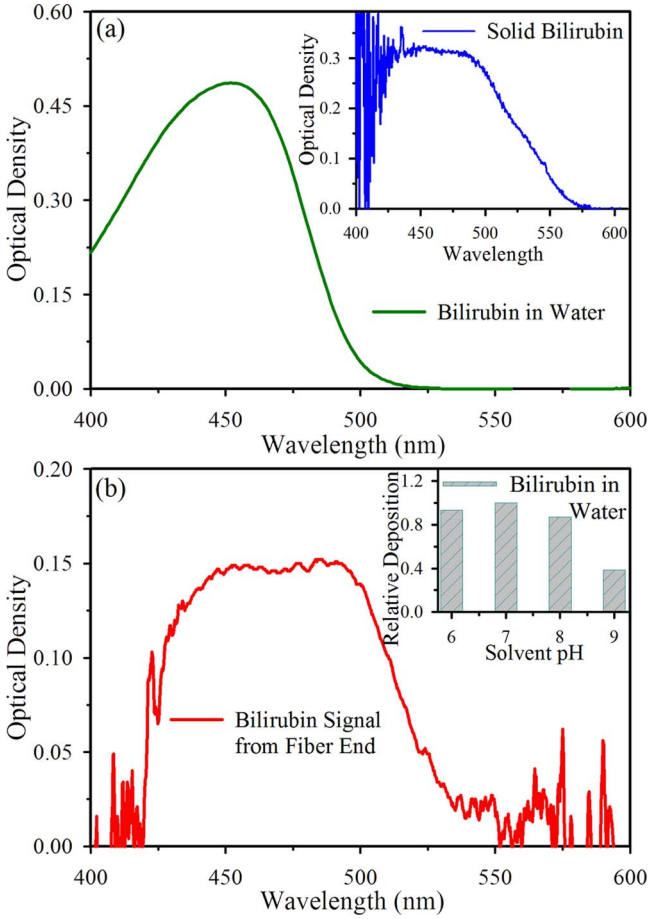

FIG. 3. (a) Absorption spectrum of bilirubin in aqueous solution (pH ~ 7.5). (b) Absorption spectrum of bilirubin solution (pH ~ 7.5) detected at the end of etched silica fiber. Similarity of the spectra with that of the solid bilirubin (inset of (a)) is clearly evident. Deposition effect of bilirubin at different pH values is shown in the inset of (b).

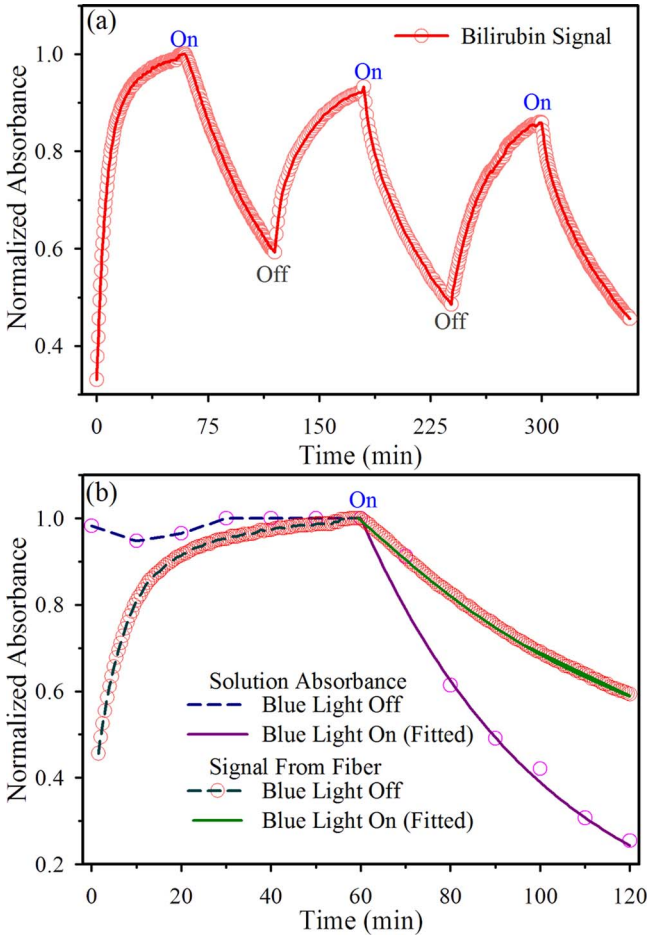

FIG. 4. (a) Time dependent absorption kinetics of aqueous bilirubin solution (12 μM, pH 7.5) as detected at the end of the silica fiber. The growth in the absence of external blue light (Off) and subsequent decay in presence of blue light (On) over three cycles is evident from the figure. (b) A comparison of the kinetics detected at the end of the silica fiber (as shown in panel (a)) by the spectrograph with that of the time dependent concentration of the same solution measured with Shimadzu-2600 spectrophotometer is demonstrated.

is directly proportional to a dimensionless parameter V,[17]

$$V = \frac{2\pi}{\lambda}\rho\sqrt{n_1^2 + n_2^2}. \quad (4)$$

Here ρ is the radius of the core and λ the wavelength of the light travelling through the fiber. For a multimode fiber the number of mode N is proportional to V^2,[17]

$$N \approx V^2. \quad (5)$$

The estimated values for N in the case of silica and 1 mm plastic fibers are $\sim 10^6$ and $\sim 10^8$, respectively. Time dependent absorption kinetics were fitted with multi-exponential function,

$$y(t) = A_1\, e^{-t/\tau_1} + A_2\, e^{-t/\tau_2} + A_3\, e^{-t/\tau_3} + y_0, \quad (6)$$

where A_i(s) are pre-exponential parameters of the corresponding exponential time constants τ_i(s). A negative value of pre-exponential function indicates growth in the kinetics. The offset y_0 is the amount of unaffected component in the kinetics within our experimental time window.

III. RESULTS AND DISCUSSION

In order to investigate the quality of the surface of optical fibers and their modification after the treatment of physical etching (silica) and heating (plastic), we have observed the fibers under scanning electron microscope (SEM). Figure 2 depicts the SEM images of the optical fibers before and after etching. From the figure, the surface of the base fibers (Figures 2(a) and 2(c)) and the modifications (Figures 2(b) and 2(d)) due to physical etching/heating is evident. It is also clear that the measured diameters of the silica and plastic fibers (223 μm and 997 μm, respectively) are consistent with the literature values provided by the manufacturer (225 μm and 1000 μm, respectively). The thickness of the clad (12 μm, Figure 2(b)) in the case of silica fiber is also similar to that of the literature value of 12.5 μm. Figure 3(a) shows absorption spectrum of aqueous bilirubin solution (9.2 μM at pH ~ 7.5) measured in Shimadzu spectrophotometer having a peak around 450 nm and consistent with reported literature.[39] In order to study the spectral response of bilirubin, white light was introduced into the fiber, the absorption spectrum of aqueous bilirubin solution (concentration 10 μM,

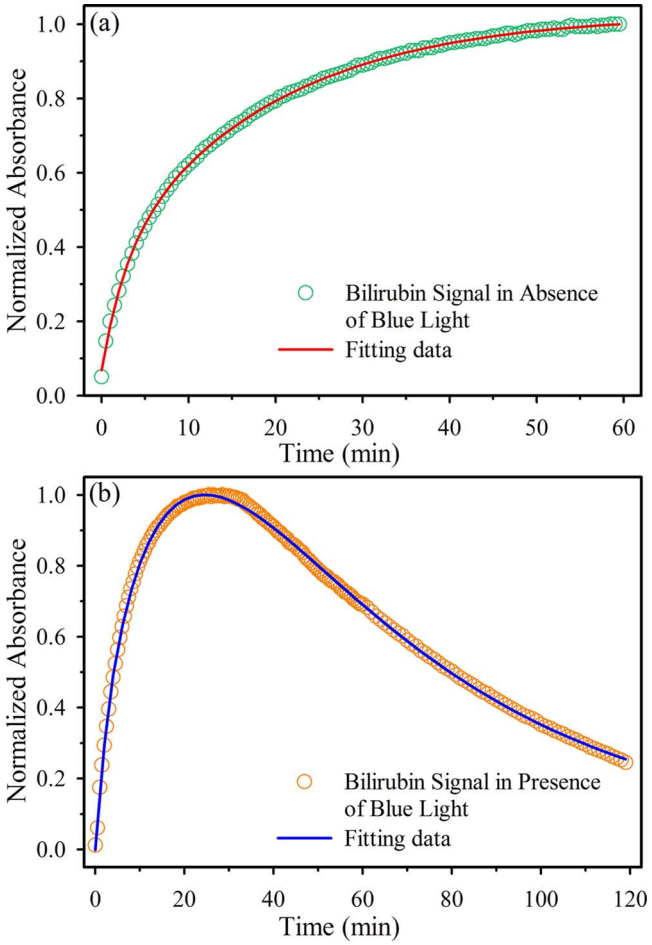

FIG. 5. Deposition of bilirubin in aqueous solution (pH 7.5, 12 μM), detected at the end of the fiber in (a) absence and (b) presence of an external blue light (1 W, 460 nm).

pH 7.5) using the spectrograph at the end of the fiber is shown in Figure 3(b). The spectra of Figures 3(a) and 3(b) are apparently looking different and the spectrum in Figure 3(b) is similar to that of the solid bilirubin as shown in the inset of Figure 3(a). The observation is consistent with the fact that the evanescent field essentially monitors solid form of bilirubin deposited at the surface of the fiber. The deposition can be rationalized from the fact that the surface of the fiber is heavily hydroxylated at pH 7.4[26] and deposition of bilirubin on the hydroxylated surface is unavoidable[18] In order to further investigate the possibility of deposition of bilirubin, we have checked the precipitation of bilirubin on a hydroxylated glass slide at different pH values. As shown in the inset of Figure 3(b), a significant amount of bilirubin can be deposited on the plate at physiological pH (7.4). It is to be noted that the deposition of bilirubin on the fiber surface may augment the evanescent field to the environments as indicated in Eq. (3), reducing the penetration depth of the probe field. In earlier studies the deposition issue of the test analytes in fiber optic sensors is concluded to be a limiting factor for the overall sensitivity of detection.[18,22,23] However, detail investigation of the deposition of the test analytes in the optical fiber sensors was beyond the scope of the earlier studies.

For the potential application of optical fiber as a theranostics tool, the deposition may work in a positive manner. The proximity of bilirubin to the evanescent field significantly increases the possibility of photodegradation of bilirubin. In our studies we have found that the spectroscopic signature of the photodegradation product is closely resemble with previously reported photo-oxidation product of bilirubin, methylvinylmaleimide (MVM).[40] After the photodegradation of bilirubin at the fiber surface, the evanescent field may "search" for new bilirubin molecule in the solution by increasing the depth of penetration (Eq. (3)). Deposition and degradation of bilirubin in aqueous solution under an external blue light (Figure 1) is shown in Figure 4. The efficacy of the optical fiber sensor to monitor the concentration of bilirubin in the solution for several cycles is demonstrated in Figure 4(a). Figure 4(b) shows a comparative study of monitoring the bilirubin concentration in solution by spectrograph in the fiber sensor, with that of the

TABLE I. Numerical fitting parameter of the bilirubin deposition (no blue light) and photo-degradation (in presence blue light) kinetics as shown in Figures 5 and 6.

Sample		Con. (μM)	y_0	A_1	τ_1 (min)	A_2	τ_2 (min)	A_3	τ_3 (min)
Silica fiber in aqueous solution (Figure 5)	Absence of blue light	10.00	0.97	−0.28	2.74	−0.70	19.71	0.08	170.57
	Presence of blue light	10.00	0.029	−0.27	2.66	−2.01	16.00	2.26	51.66
Bilirubin deposition/degradation on silica fiber (no blue light)	Figure 6(a)	11.04	1.02	−0.27	3.22	−0.51	40.00	0.10	200.00
	Figure 6(b)	19.14	0.96	−0.23	0.78	−0.67	22.40	0.10	200.00
	Figure 6(c)	29.08	0.96	−0.23	0.77	−0.66	22.26	0.10	200.00
	Figure 6(d)	36.04	0.95	−0.27	2.63	−0.71	19.32	0.10	196.43
	Figure 6(e)	35.64	1.03	−0.39	3.92	−0.76	30.28	0.10	186.61
Bilirubin deposition/degradation on silica fiber (in blue light)	Figure 6(a)	11.04	0.00	−0.20	3.2	−0.1	40.00	6.15	33.51
	Figure 6(b)	19.14	0.00	−1.55	1.34	−3.23	17.98	2.00	103.03
	Figure 6(c)	29.08	0.00	−0.03	2.95	−1.32	30.79	1.81	150.00
	Figure 6(d)	36.04	0.00	−0.20	2.30	−0.34	27.33	1.27	289.70
	Figure 6(e)	35.64	0.00	−0.79	4.79	−1.07	14.06	1.15	472.00

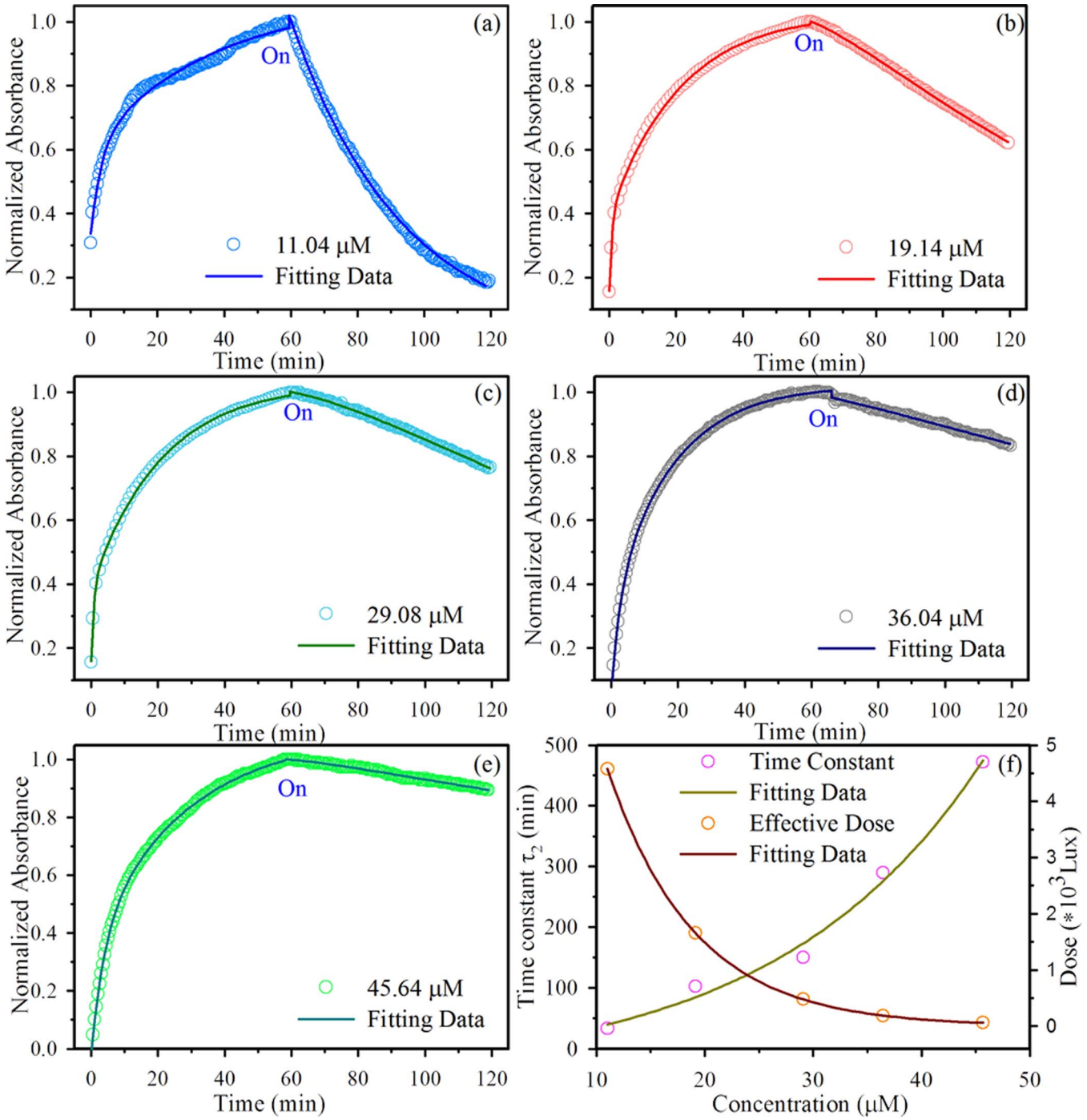

FIG. 6. Concentration dependent deposition and degradation (in absence and presence of blue light) of bilirubin as detected by fiber (panel (a)–(e)). Dominance of degradation kinetics in presence of blue light is evident. Panel (f) shows slower degradation with high bilirubin concentration. The effective dose of light at the fiber surface with bilirubin concentration is also shown.

readings obtained from Shimadzu spectrophotometer. From Figure 4(b) it is evident that the spectrophotometer unable to monitor the deposition of the bilirubin, which is very local effect at the surface of the fiber only, however, very important for the sensing efficiency. Numerical fitting of the deposition (Figure 4(b)) in absence of light reveal exponential rise of time constant 21.00 min. In presence of blue light the decay kinetics can be fitted with bi-exponential function with a rise component of 21.00 min followed by a decay of time constant 42.05 min with residual component (y_0) of 0.46. It has to be noted that the kinetics measured with the spectrophotometer can be fitted with a single exponential decay with time constant of 42.44 min, which is consistent with the decay component measured with spectrograph ($\tau_2 = 42.00$ min). The observation reveals that fiber sensor attached with the spectrograph measures similar decay kinetics, convoluted with a rise component due to the deposition of bilirubin at the surface and invites care for the interpretation of kinetics data from a fiber sensor used to measure concentration of an analyte in solution phase.

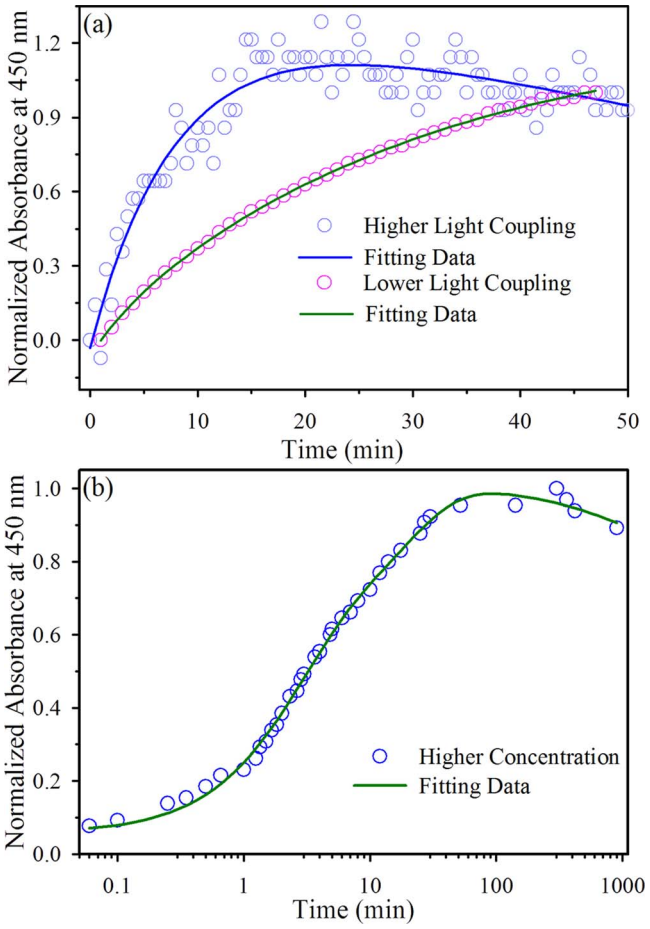

FIG. 7. Efficacy of the setup in potential theranostics application is demonstrated in a prototype experiment. It is clear from Figures 7(a) and 7(b) that degradation of bilirubin depends on the amount of light coupled to the silica fiber.

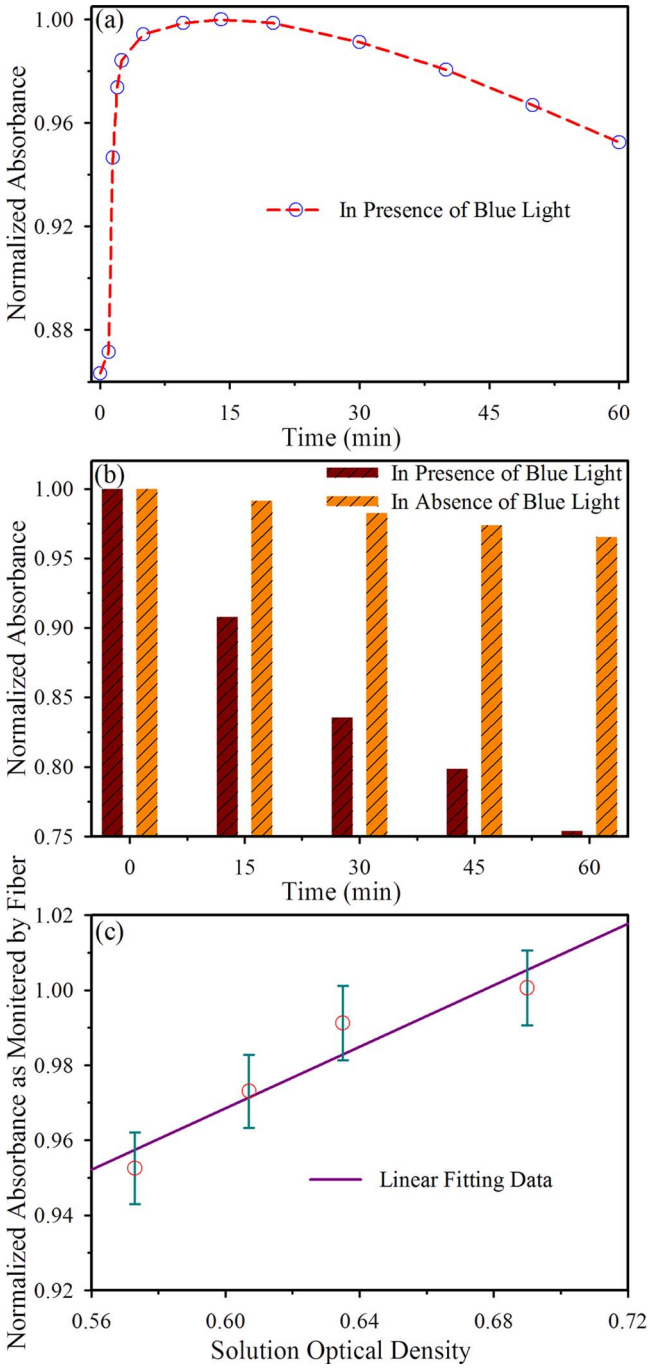

FIG. 8. The theranostics applicability of the prototype is represented using 1 mm fiber as sensor and Coherent FieldMate with OP-2 VIS sensor as detector. (a) The detected signal from the fiber end. (b) Comparative solution concentration measured in Shimadzu spectrophotometer in presence and absence of blue light. (c) The linear dependency between the signals detected at the fiber end and the solution concentration.

In order to investigate the deposition effect on the surface of the fiber, we have studied the signal from the fiber sensor in absence and presence of external blue light source, as shown in Figures 5(a) and 5(b). Table I represents the fitting kinetics data. It is clear that deposition is also an integral part of the decay kinetics and needs numerical fitting for the interpretation of the kinetics. The deposition and degradation (in absence and presence of blue light) of bilirubin at various concentrations is shown in Figure 6. Corresponding kinetics data is tabulated in Table I. As evident from Table I and Figure 6(f), with increasing concentration of bilirubin, the decay kinetics gradually become slower. This observation can be rationalized in term of our experimental setup (Figure 1), revealing lowers effective dose of light at the fiber surface with the increase in solution concentration (inner filter effect). From Figure 6 and corresponding fitting data in Table I, it is also clear that the rise time constants almost remain unperturbed in the range of solution concentrations in our study. While the faster rise time constants 2–4 min may be consistent with homogenization of the solution, long time constants in the range of 20–40 min account for deposition of bilirubin at the fiber surface.

In real theranostics application there is very little scope to use external light source rather use of the light through the fiber for both sensing and phototherapy. Figure 7 shows the efficacy of the setup, in which a blue LED is coupled to the etched silica fiber and the transmitted optical power is detected by a spectrograph (Figure 7(a)) and a power meter (Figure 7(b)). It is evident from Figure 7(a), the degradation depends on the amount of power coupled to the fiber which can be differentiated in terms of light intensity at the detector end of the fiber. Although, sensing of bilirubin is

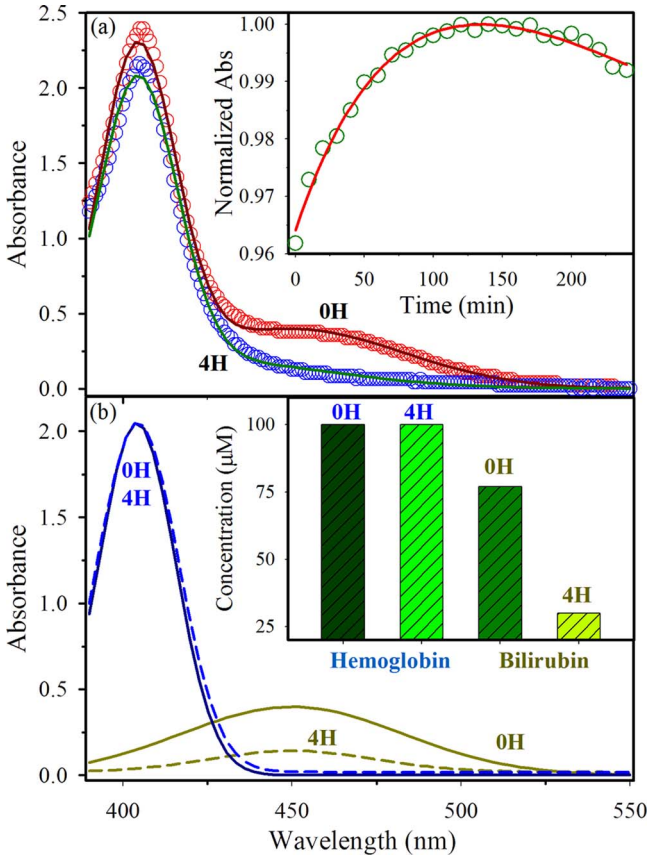

FIG. 9. (a) Absorption spectra of bilirubin (77 μM/l) in blood-phantom (HSA and hemoglobin mixture) solution before (0 H) and after 4 hours of photodegradation (4 H) by blue LED evanescent field. Solid lines indicate the goodness of spectral deconvolution the experimental data with two peaks at 404 nm (soret band of hemoglobin) and 450 nm (bilirubin). The inset represents time dependence of detected absorbance signal at the fiber end. Initial rise in the signal depicts the dominance of deposition of bilirubin and following photodegradationt leads the consequent decrease. (b) The deconvoluted spectra peaking at 404 nm (soret band of hemoglobin) and 450 nm (bilirubin) before and after the photo (450 nm) irradiation of the blood phantom are shown. Inset shows a clear decrease in the bilirubin (estimated value from 77 μM/l to 30 μM/l) and intactness of hemoglobin concentration.

irrespective of the coupling efficiency, bilirubin degradation very much depends on the coupled light to the fiber. In our experimental condition (e.g., fiber end polishing, surface etching) the coupling efficiency varies revealing output power of the blue LED light at the fiber end in the range of 22–25 μW (higher coupling) to 4–5 μW (lower coupling). Figure 7(b) clearly indicates that for moderately coupled systems someone has to wait significant amount of time in order to get reasonable degradation effect. This observation clearly justify the increased amount of modes (higher V number; Eq. (2)) coupled to the optical fiber for potential application in theranostics. Figure 8 shows the data obtained using plastic fiber of diameter 1 mm. As shown in Figures 8(a) and 8(b), a significant amount of photodegradation can be achieved in 60 min. It has to be noted that we have calibrated the concentration of bilirubin measured by the fiber sensor with that measured using spectrophotometer. In 60 min of experimental time span we have found reasonable linearity (Figure 8(c)), revealing the reliability of the data reported by the fiber sensor. In order to address the specific question, whether the sensor able to degrade bilirubin up to clinically meaningful amount in a physiologically relevant environment so that it can be actually used for therapy, we have studied the photodegradation of bilirubin in a mixture of HSA and Hemoglobin (100 μM/l of each protein), two major ingredients of human blood. As shown in Figure 9(a), the removal of bilirubin from the "blood-phantom" solution is significant revealing bilirubin degradation from 77 μM/l to 30 μM/l. It has to be noted that the level of bilirubin in the human blood in normal and jaundice conditions are ~20 μM/l and >50 μM/l, respectively. The spectral deconvolution of the absorption spectra (solid lines) in the range from 390 nm to 550 nm shows the presence of hemoglobin (soret band peak at 404 nm) and bilirubin (peak at 450 nm). The peak of HSA is supposed to be at 280 nm and beyond the spectral range. The deposition followed by the degradation measured from the optical power meter is clear from the inset of Figure 9(a). The deconvoluted spectra peaking at 404 nm (hemoglobin) and 450 nm (bilirubin) at different time of irradiation are shown in Figure 9(b). A clear decrease of the spectrum peaking at 450 nm with time, as a consequence of photodegradation of bilirubin is evident from the inset Figure 9(b) without affecting the hemoglobin count in the blood-phantom. Our observation further justifies the potentiality of our strategy for novel theranostics tool in future applications.

The promising experimental observation as shown in Figures 8 and 9, directed us for an *in vitro* theranostics application on a wet-chromatography paper as membrane mimic. Cellulose or polysaccharides are the primary constituent of chromatography paper, which are also the major components of fibrous extracellular matrix of skin dermis of green plants, many forms of algae and eukaryotic microorganisms. Thus in order to effectively simulate the structure and composition of native skin, we have used wet-chromatography paper. Since, cellulose is significantly amphiphilic in nature, incorporation of bilirubin (which is generally considered as a lipophilic substance) in to the chromatography paper is primarily governed by the lipophilic or hydrophobic interactions.[41–43] The experimental setup for the *in vitro* studies is shown in Figure 10(a). The experimental data on the bilirubin degradation measured with power meter (Figure 10(b)) and spectrophotometer (Figure 10(c)) are shown. From both the model experiments, it is clear that the degradation monitored by the power meter is apparent after sufficient photodegradation of the test pigment in the solution as monitored by the spectrophotometer. Continuous deposition of the bilirubin on the plastic fiber surface is concluded to be reason for such observation. In a separate experiment on the deposition of bilirubin on the plastic fiber (data not shown), a time constant of 46.00 min is evident. It has to be noted that the degradation time constant is also in the similar order as monitored from spectrophotometer (Figures 8(b) and 10(c)). The model experiments also suggest that concentration monitored by the power-meter at the end of the fiber starts showing the decrease of bilirubin level in test medium, when the concentration of the pigment is significantly lower than the starting value. The observation clearly reveals the efficacy of continuous monitoring the level of bilirubin in the test environments during phototherapy.

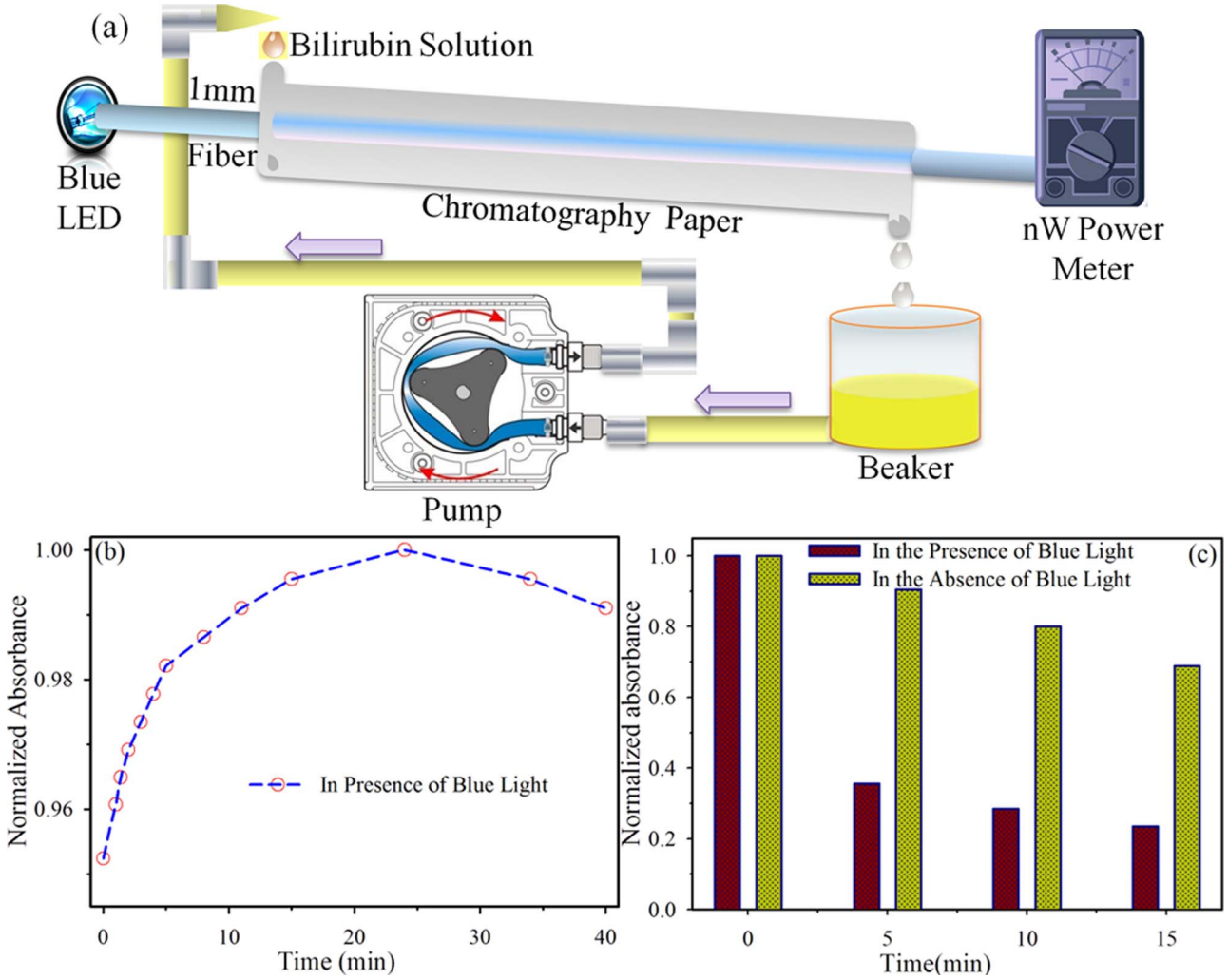

FIG. 10. The *in vitro* theranostics application for hyperbilirubinemia is represented using 1 mm fiber as sensor and Coherent FieldMate with OP-2 VIS sensor as detector. (a) The schematic presentation of the experimental setup. (b) The signal detected at the Fiber end by the power meter. (c) The comparative solution concentration measured in Shimadzu spectrophotometer in presence and absence of blue light.

IV. CONCLUSION

In the present study, we have developed a fiber optic evanescent field-based sensor for the detection of bilirubin in an aqueous medium. Our pH dependent studies show the efficacy of our developed fiber sensor depends on the deposition of bilirubin on the fiber surface due to the presence of unavoidable hydroxyl moieties on the silica surface. Our studies clearly reveal the importance of numerical fitting considering the deposition effect on the kinetics data obtained from the fiber sensor. We have demonstrated the efficacy of our strategy in the maintenance of controlled bilirubin level in a blood-phantom solution (mixture of hemoglobin and HSA). We have also shown that bilirubin deposited at the fiber surface can be removed using the evanescent field. In a prototype experiment we have designed a way to detect the level of bilirubin (diagnosis) and its photodegradation (therapy) simultaneously, using a single fiber. The method could be useful for both noninvasive (on skin, like phototherapy) and invasive (in contact with blood); however, actual therapeutic strategy may be determined after a rigorous clinical trial. Apart from its fundamental importance, we believe that this work represents a step forward in the use of evanescent field (light) for potential theranostics application in hyperbilirubinemia.

ACKNOWLEDGMENTS

N.P. thanks DST, India for Inspire Research Fellowship. We thank DST, India for financial grants (DST/TM/SERI/2k11/103 & SB/S1/PC-011/2013).

[1]D. O. Lapotko, Theranostics **3**, 138 (2013).
[2]D. H. Sliney and S. L. Trokel, *Medical Lasers and Their Safe Use* (Springer-Verlag, New York, 1993).
[3]S. K. Houston, C. C. Wykoff, A. M. Berrocal, D. J. Hess, and T. G. Murray, Laser Med. Sci. **28**, 683 (2013).
[4]R. H. Chmait, L. M. Korst, A. Llanes, P. Mullin, R. H. Lee, and J. G. Ouzounian, Am. J. Obstet. Gynecol. **209**, 264.e1 (2013).
[5]K. Kong, C. J. Rowlands, S. Varma, W. Perkins, I. H. Leach, A. A. Koloydenko, H. C. Williams, and I. Notingher, Natl. Acad. Sci. **110**, 15189 (2013).
[6]X. Wu, H. Liu, J. Liu, K. N. Haley, J. A. Treadway, J. P. Larson, N. Ge, F. Peale, and M. P. Bruchez, Nat. Biotechnol. **21**, 41 (2002).
[7]H. Zhang, D. Yee, and C. Wang, Nanomedicine **3**, 83 (2008).
[8]G. Luo, J. Long, B. Zhang, C. Liu, S. Ji, J. Xu, X. Yu, and Q. Ni, Expert Opin. Drug Delivery **9**, 47 (2012).

[9]S. Sarkar, A. Makhal, S. Baruah, M. A. Mahmood, J. Dutta, and S. K. Pal, J. Phys. Chem. C **116**, 9608 (2012).
[10]G. J. Tearney, M. E. Brezinski, B. E. Bouma, S. A. Boppart, C. Pitris, J. F. Southern, and J. G. Fujimoto, Science **276**, 2037 (1997).
[11]R. R. Alfano, AIP Adv. **2**, 011103 (2012).
[12]J. M. Edmonson, Gastrointest. Endosc. **37**, S27 (1991).
[13]N. Abe, H. Takeuchi, A. Ooki, G. Nagao, T. Masaki, T. Mori, and M. Sugiyama, Dig. Endosc. **25**, 64 (2013).
[14]K. Yao, G. Anagnostopoulos, and K. Ragunath, Endoscopy **41**, 462 (2009).
[15]P. H. Paul and G. Kychakoff, Appl. Phys. Lett. **51**, 12 (1987).
[16]V. Ruddy, B. D. MacCraith, and J. A. Murphy, J. Appl. Phys. **67**, 6070 (1990).
[17]A. Leung, P. M. Shankar, and R. Mutharasan, Sens. Actuators, B **125**, 688 (2007).
[18]A. Armin, M. Soltanolkotabi, and P. Feizollah, Sens. Actuators, A **165**, 181 (2011).
[19]C. Beres, F. V. B. de Nazaré, N. C. C. de Souza, M. A. L. Miguel, and M. M. Werneck, Biosens. Bioelectron. **30**, 328 (2011).
[20]M. N. Velasco-Garcia, Sem. Cell Dev. Biol. **20**, 27 (2009).
[21]C. Ciminelli, C. M. Campanella, F. Dell'Olio, C. E. Campanella, and M. N. Armenise, Prog. Quantum Electron. **37**, 51 (2013).
[22]A. Safaai-Jazi and J. V. Petersen, Opt. Laser Technol. **26**, 399 (1994).
[23]P. K. Choudhury and T. Yoshino, Optik **115**, 329 (2004).
[24]T. A. Russell, U.S. patent 6,290,713 B1 (18 September 2001).
[25]C. B. Allen, B. K. Schneider, and C. W. White, Am. J. Physiol.: Lung Cell Mol. Physiol. **281**, L1021 (2001).
[26]B.-C. Deboux, E. Lewis, P. Scully, and R. Edwards, J. Lightwave Technol. **13**, 1407 (1995).
[27]A. B. Ganesh and T. Radhakrishnan, Fiber Integr. Opt. **25**, 403 (2006).
[28]E. Li, X. Wang, and C. Zhang, Appl. Phys. Lett. **89**, 091119 (2006).
[29]J. Ostrow, *Bile Pigments and Jaundice: Molecular, Metabolic, and Medical Aspects* (Marcel Dekker Inc, New York, 1986).
[30]M. J. Maisels and A. F. McDonagh, N. Engl. J. Med. **358**, 920 (2008).
[31]R. Cremer, P. Perryman, and D. Richards, Lancet **271**, 1094 (1958).
[32]D. A. Lightner and A. F. McDonagh, Acc. Chem. Res. **17**, 417 (1984).
[33]A. A. Lamola, W. E. Blumberg, R. McClead, and A. Fanaroff, Proc. Natl. Acad. Sci. U.S.A. **78**, 1882 (1981).
[34]S. E. Braslavsky, A. R. Holzwarth, and K. Schaffner, Angew. Chem., Int. Ed. **22**, 656 (1983).
[35]P. F. Sebbe, A. G. J. B. Villaverde, R. A. Nicolau, A. M. Barbosa, and N. Veissid, AIP Conf. Proc. **992**, 606 (2008).
[36]S. K. Khijwania and B. D. Gupta, Opt. Quant. Electron. **31**, 625 (1999).
[37]D. J. Griffiths, *Introduction to Electrodynamics* (Prentice Hall, New Jersey, 1999).
[38]J. D. Jackson, *Classical Electrodynamics* (Wiley, Singapore, 1975).
[39]G. Blauer and T. E. King, J. Biol. Chem. **245**, 372 (1970).
[40]W. E. Kurtin, Photochem. Photobiol. **27**, 503 (1978).
[41]M. B. Sticklen, Nat. Rev. Genet. **9**, 433 (2008).
[42]B. Medronho, A. Romano, M. Miguel, L. Stigsson, and B. Lindman, Cellulose **19**, 581 (2012).
[43]E. Vatankhah, M. P. Prabhakaran, G. Jin, L. G. Mobarakeh, and S. Ramakrishna, J. Biomater. Appl. **28**, 909 (2014).